ArXiv: astro-ph, Dec 14-18, 2015

От Сильченко О.К.

Astro-ph: 1512.04264

The XXL Survey ⋆,⋆⋆

II. The bright cluster sample: catalogue and luminosity function

F. Pacaud[1], N. Clerc[2], P. A. Giles[3], C. Adami[4], T. Sadibekova[5], M. Pierre[5], B. J. Maughan[3], M. Lieu[6], J. .P. Le Fèvre[7], S. Alis[8,9], B. Altieri[10], F. Ardila[11], I. Baldry[28], C. Benoist[9], M. Birkinshaw[3], L. Chiappetti[12], J. Démoclès[6,5], D. Eckert[13], A. E. Evrard[14], L. Faccioli[5], F. Gastaldello[12], L. Guennou[15], C. Horellou[17], A. Iovino[18], E. Koulouridis[19,5], V. Le Brun[4], C. Lidman[16], J. Liske[29], S. Maurogordato[9], F. Menanteau[20], M. Owers[21,16], B. Poggianti[22], D. Pomarède[7], E. Pompei[23], T. J. Ponman[6], D. Rapetti[24,25], T. H. Reiprich[1], G. P. Smith[6], R. Tuffs[30], P. Valageas[26], I. Valtchanov[10], J. P. Willis[27], and F. Ziparo[6]

(Affiliations can be found after the references)

XMM Newton: Поле обзора: 25x2 кв. градуса

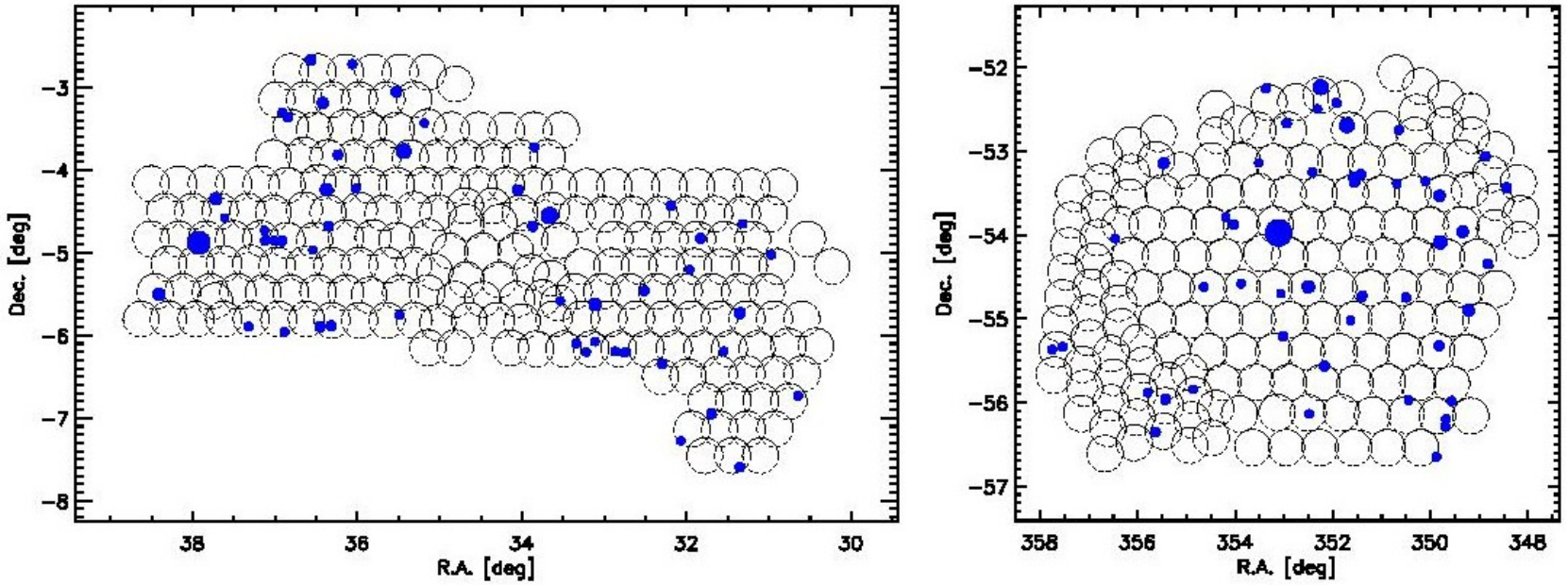

Fig. 1. Sky distribution of the XXL pointings that passed the selection criteria for the construction of the cluster sample. The dashed circles represent the area used for cluster detection on each pointing, i.e. a 13′ radius around the average optical axis. The location of the members of the bright XXL cluster sample is shown with blue dots, whose size is proportional to their 60″ aperture flux. The ~ 1 deg^2 area located around RA=34.5 and Dec =-5, is the Subaru Deep Survey, whose position was selected for its lack of bright X-ray sources.

Оптическое отождествление, распределение по массам и z

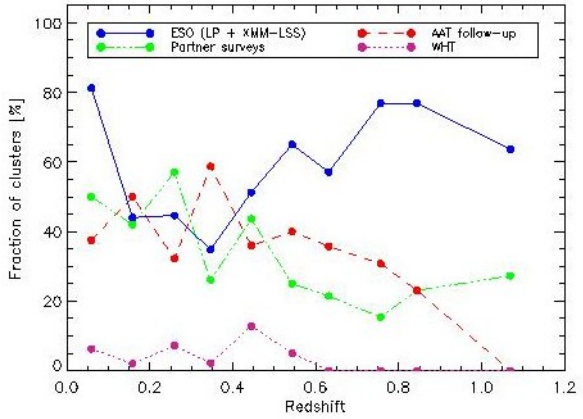

Fig. 3. Origin of the XXL-100-GC sample spectroscopic redshifts in different redshift slices. The available spectroscopic data are split into four categories: (i) the follow-up data obtained by the dedicated XXL ESO Large Program (LP, PI: C. Adami) using a combination of NTT/EFOSC2 and VLT/FORS2, together with previous data obtained by the XMM-LSS team with the same instruments, (ii) the XXL follow-up program based on the the Anglo-Australian Telescope (AAT, PI: C. Lidman), (iii) the XXL William Herschel Telescope (WHT) follow-up program (PI: B. Poggianti), and (iv) redshifts obtained through partner spectroscopic surveys, including GAMA (Driver et al. 2011), VIPERS (Garilli et al. 2014) and the VVDS (Le Fèvre et al. 2013). The observa-

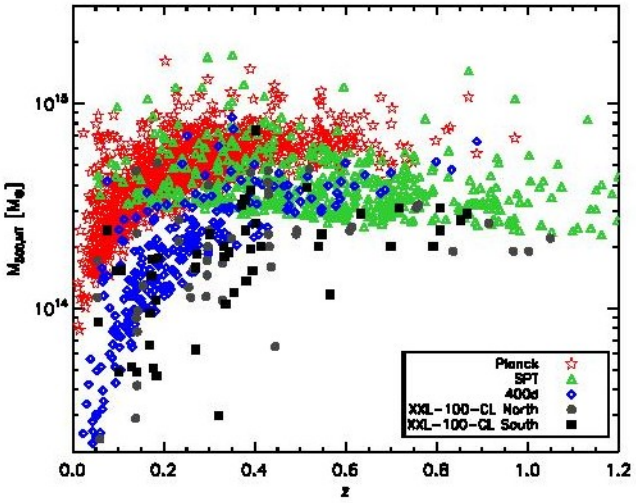

Fig. 8. Comparison of the mass and redshift distribution of the bright XXL cluster sample with other cluster samples. We detect on average lower-mass / higher-redshift clusters than current Sunyaev-Zel'dovich cluster surveys (Bleem et al. 2015; Planck Collaboration et al. 2015a), as well as the 400 deg^2 ROSAT survey based on deep archival pointings. At high redshift, the selection of the XXL-100-GC sample is also much closer to being mass-limited than for ROSAT-based surveys such as the 400d.

Рассогласование с космологией

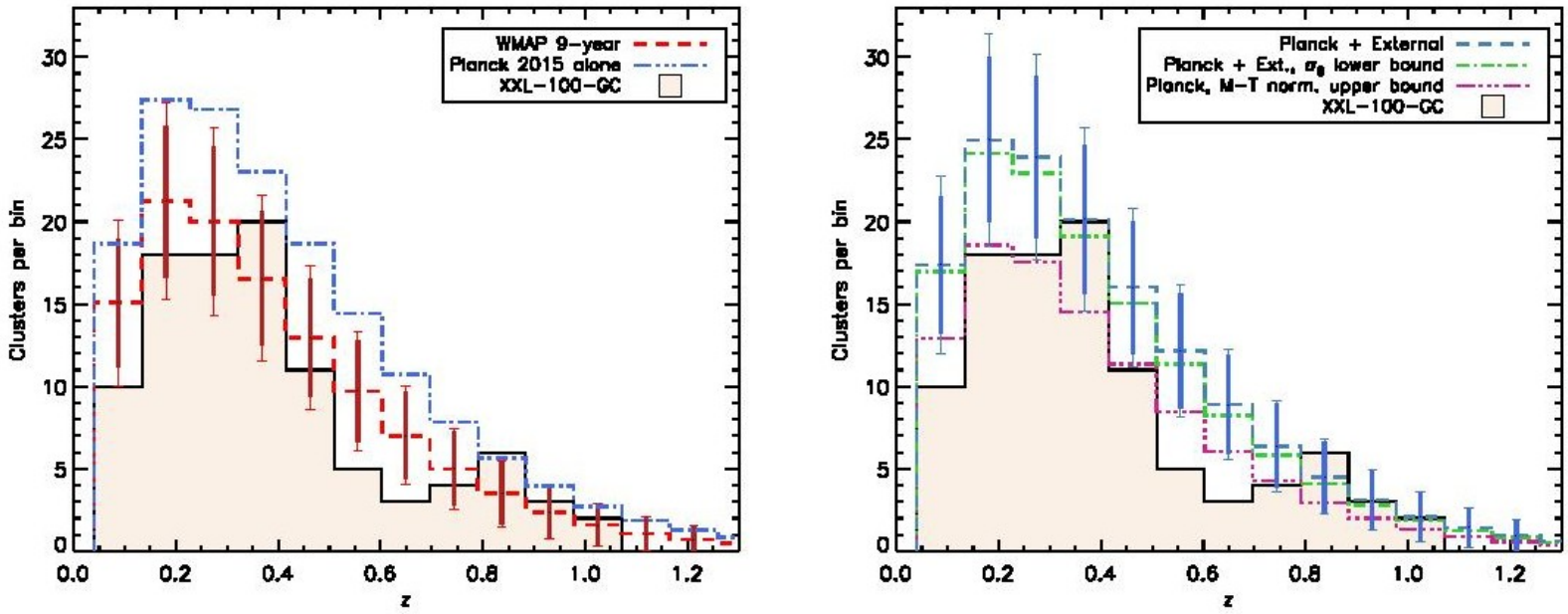

Fig. 11. Redshift distribution of the XXL-100-GC sample (filled histogram) compared with different model expectations. By default, the model predictions are based on the mass and temperature scaling relations of Paper III and Paper IV, and assume a β-model with $\beta = 2/3$ and $x_{500} = 0.15$. *Left*: The fiducial WMAP9 cosmology (red dashed line) compared with the *Planck* 2015 cosmological parameters obtained only from the CMB data (blue dot-dashed). *Right*: Other models derived from Planck Collaboration et al. (2015b). The *Planck*+External set of cosmological parameters includes additional BAO and H0 constraints (blue dashed). The green dot-dashed line is the same, but fixing σ_8 to the 1σ lower bound allowed by the *Planck*+External data set. The purple triple dot-dashed line uses the *Planck*-only parameters, but the normalisation of the $M_{500,WL} - T_{300kpc}$ scaling relation has been increased to its 1σ upper bound. The error bars (shown only for the WMAP9 and *Planck*+External cosmologies) include both the shot noise (thick part) and the cosmic variance.

Рассогласование с космологией: предсказание WMAP (9 yr)

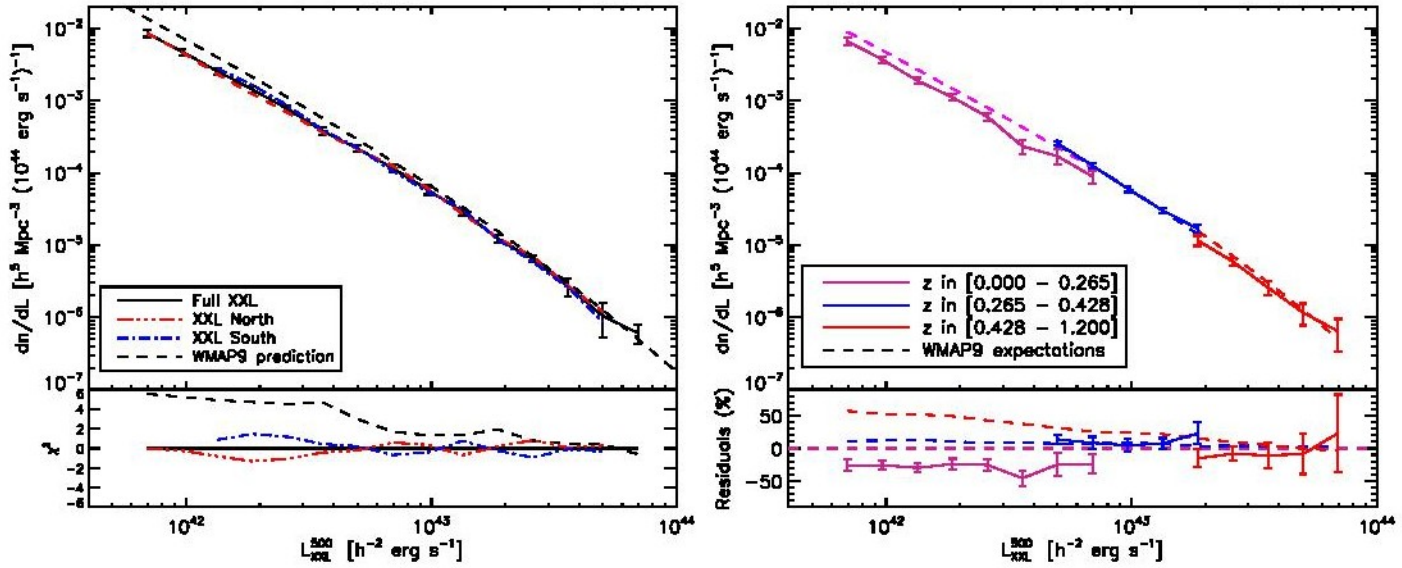

Fig. 12. Differential luminosity function of the XXL-100-GC sample in the WMAP9 cosmology measured with the cumulative estimator defined by Eq. (7). The effective volume correction derives from the XXL-100-GC scaling relations provided in Table 1. The dashed lines show the predictions of the luminosity function in the WMAP9 cosmological model for the same redshift bins as the measurements, and using the same colour code. *Left*: Differential luminosity function averaged over the full redshift range of [0-1.2] covered by the XXL-100-GC sample, and for the northern/southern field separately. The χ^2 plot shows how the deviation of each subfield from the complete analysis compares with the combined error bars. *Right*: Differential luminosity function of the bright XXL cluster sample in three redshift bins. The lower plot shows the residuals with respect to the low-redshift WMAP9 prediction.

Astro-ph: 1512.03814

The XXL Survey*
XIII. Baryon content of the bright cluster sample

D. Eckert[1,2], S. Ettori[3,4], J. Coupon[1], F. Gastaldello[2], M. Pierre[5], J.-B. Melin[6], A. M. C. Le Brun[5,7], I. G. McCarthy[7], C. Adami[8], L. Chiappetti[2], L. Faccioli[5], P. Giles[9], S. Lavoie[10], J. P. Lefèvre[11], M. Lieu[12], A. Mantz[13], B. Maughan[9], S. McGee[12], F. Pacaud[14], S. Paltani[1], T. Sadibekova[5], G. P. Smith[12], and F. Ziparo[12]

Доля барионов в звездах и газе

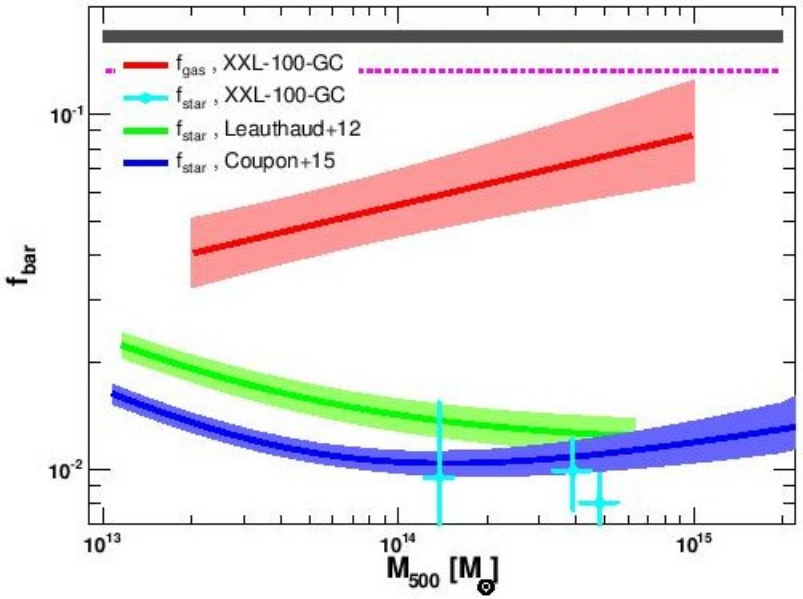

Fig. 7. Baryon fraction in the form of hot gas (red, this work) and stars. The cyan data points show the measurements obtained for the XXL-100-GC sample in three temperature bins (see Table 1), compared to literature measurements at different redshifts ($z \sim 0.3$, Leauthaud et al. (2012, green); $z \sim 0.8$, Coupon et al. (2015, blue)). The WMAP9 cosmic baryon fraction is displayed in the grey shaded area, whereas the dashed magenta line indicates the cosmic baryon fraction corrected by the depletion factor $Y_b = 0.85$ at r_{500} (Planelles et al. 2013).

Доля барионов в газе: рассогласование с космологией, нет гидростатике!

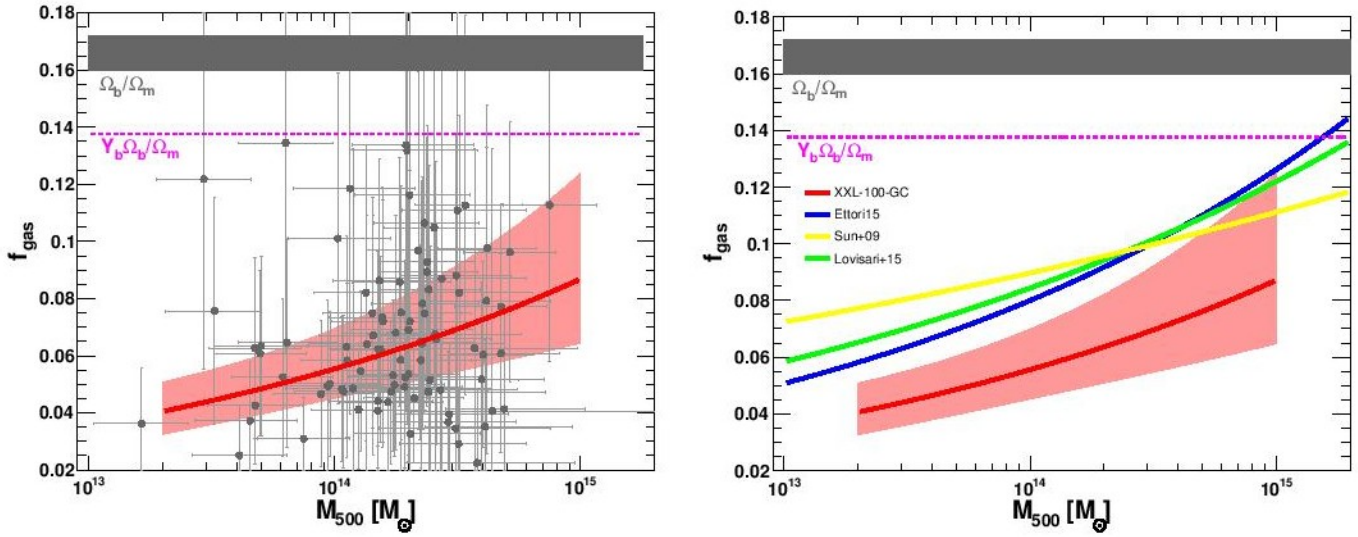

Fig. 4. Relation between gas fraction and halo mass within $r_{500,MT}$ for the XXL-100-GC sample. *Left:* The red line and the red shaded area show the best-fit relation and its uncertainty. The data points show the individual f_{gas} estimates obtained using the $M-T$ relation. The WMAP9 cosmic baryon fraction is displayed in the grey shaded area, whereas the dashed magenta line indicates the cosmic baryon fraction corrected by the depletion factor $Y_b = 0.85$ at r_{500} (Planelles et al. 2013). *Right:* Same as in the left panel. For comparison, the solid curves show similar relations obtained using hydrostatic masses (yellow, Sun et al. (2009); blue, Ettori (2015); green, Lovisari et al. (2015)).

Astro-ph: 1512.04543

THE SMALL SCATTER OF THE BARYONIC TULLY-FISHER RELATION

FEDERICO LELLI[1], STACY S. MCGAUGH[1], JAMES M. SCHOMBERT[2]

Draft version December 16, 2015

ABSTRACT

In a ΛCDM cosmology, the baryonic Tully-Fisher relation (BTFR) is expected to show significant intrinsic scatter resulting from the mass-concentration relation of dark matter halos and the baryonic-to-halo mass ratio. We study the BTFR using a sample of 118 disc galaxies (spirals and irregulars) with data of the highest quality: extended H I rotation curves (tracing the outer velocity) and Spitzer photometry at 3.6 μm (tracing the stellar mass). Assuming that the stellar mass-to-light ratio (Υ_*) is nearly constant at 3.6 μm, we find that the scatter, slope, and normalization of the BTFR systematically vary with the adopted Υ_*. The observed scatter is minimized for $\Upsilon_* \gtrsim 0.5$ $M_\odot/L_\odot$, corresponding to nearly maximal discs in high-surface-brightness galaxies and BTFR slopes close to ∼4. For any reasonable value of Υ_*, the intrinsic scatter is ∼0.1 dex, below general ΛCDM expectations. The residuals show no correlations with galaxy structural parameters (radius or surface brightness), contrary to the predictions from some semi-analytic models of galaxy formation. These are fundamental issues for ΛCDM cosmology.

Subject headings: galaxies: kinematics and dynamics — galaxies: formation — galaxies: evolution — galaxies: spiral — galaxies: irregular — dark matter

Барионное Талли-Фишера: разброса точек просто нет!

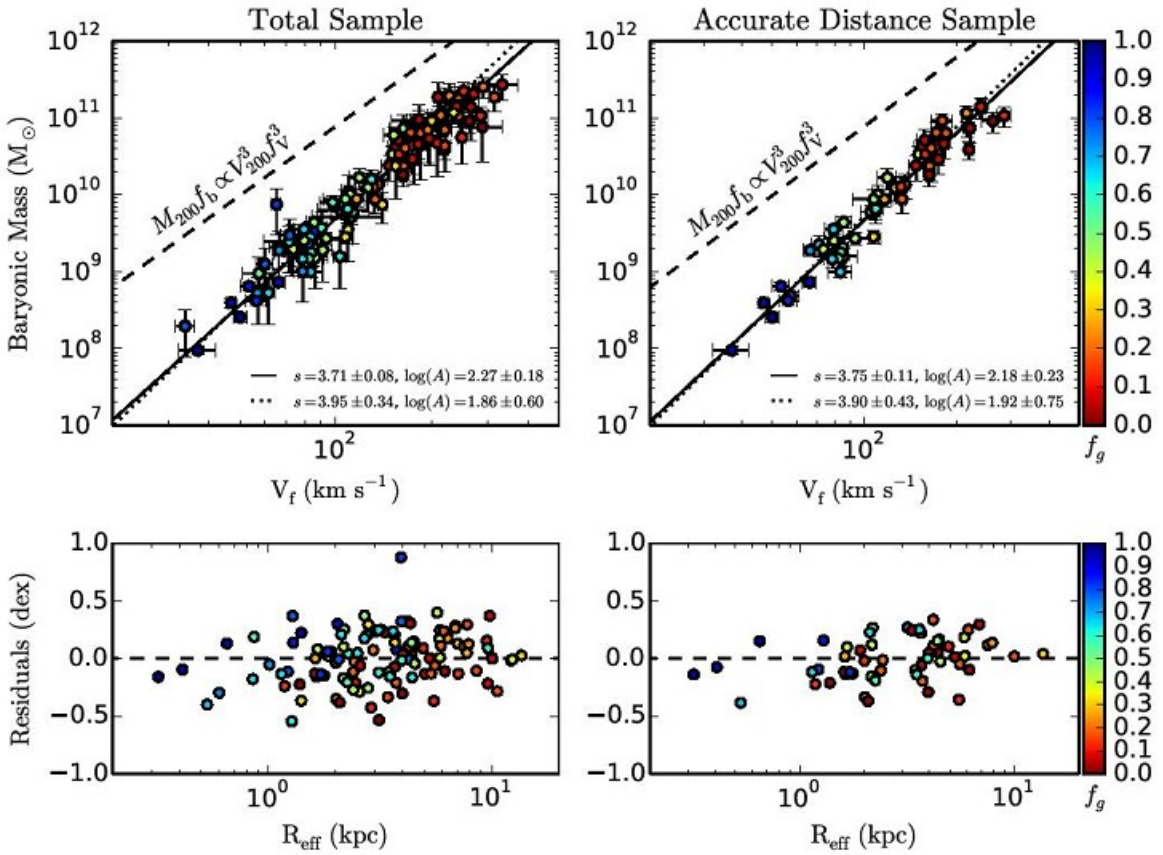

FIG. 2.— *Top panels*: BTFR adopting $\Upsilon_* = 0.5\ M_\odot/L_\odot$. Galaxies are color-coded by $f_g = M_g/M_b$. Solid lines show error-weighted fits. Dotted lines show fits weighted by f_g^2, increasing the importance of gas-dominated galaxies. The dashed line shows the ΛCDM initial condition with $f_V = 1$ and $f_b = 0.17$ (the cosmic value). *Bottom panels*: residuals from the error-weighted fits versus the galaxy effective radius. The outlier is UGC 7125, which has an unusually high correction for Virgocentric infall and lies near the region where the infall solution is triple-valued. If we consider only the correction for Local Group motion, UGC 7125 lies on the BTFR within the scatter.